Novel selective agents for the degradation of androgen receptor variants to treat castration-resistant prostate cancer

Suriyan Ponnusamy[1], Christopher C. Coss[2,#], Thirumagal Thiyagarajan[1], Kate Watts[3], Dong-Jin Hwang[4], Yali He[4], Luke A. Selth[5,6], Iain J. McEwan[3], Charles B. Duke[4,@], Jayaprakash Pagadala[4], Geetika Singh[7], Robert W. Wake[8], Christopher Ledbetter[8], Wayne D. Tilley[5,6], Tudor Moldoveanu[7], James T. Dalton[2,^], Duane D. Miller[4], and Ramesh Narayanan[1,9,*]

[1] Department of Medicine, The University of Tennessee Health Science Center, Memphis, TN
[2] GTx, Inc., Memphis, TN
[3] School of Medicine, Medical Sciences and Nutrition, Institute of Medical Sciences, University of Aberdeen, Aberdeen AB25 2ZD, Scotland, UK
[4] Department of Pharmaceutical Sciences, The University of Tennessee Health Science Center, Memphis, TN
[5] Dame Roma Mitchell Cancer Research Laboratories, School of Medicine, The University of Adelaide, SA 5005 Australia
[6] Freemasons Foundation Centre for Men's Health, School of Medicine, The University of Adelaide, SA 5005 Australia
[7] St. Jude Children's Hospital and Research Center, Memphis, TN
[8] Department of Urology, The University of Tennessee Health Science Center, Memphis, TN
[9] West Cancer Center, Memphis, TN

[#] Current address: College of Pharmacy, Ohio State University, Columbus, OH
[^] Current address: College of Pharmacy, University of Michigan, Ann Arbor, MI
[@] Current address: Department of Emergency Medicine, Yale School of Medicine, New Haven, CT

* Address correspondence to:
Dr. Ramesh Narayanan
Department of Medicine
Division of Hematology and Oncology
The University of Tennessee Health Science Center
Cancer Research Building
19 S. Manassas, Room 120
Memphis, TN- 38103
Phone 901-448-2403
Fax 901-448-3910
rnaraya4@uthsc.edu

Running title: SARDs for the treatment of prostate cancer
Key words: Androgen Receptor (AR), Selective Androgen Receptor Degraders (SARDs), AR Splice Variants (AR-SV), prostate cancer, Castration-Resistant Prostate Cancer (CRPC), AR antagonist, AF-1-binding AR antagonist, AR translocation inhibitor, AR pan-antagonist.
Funding Source: The research presented in this manuscript was supported by a research funding provided by GTx, Inc. Memphis, TN to R. Narayanan and by a research funding provided by West Cancer Center to R. Narayanan.
Disclosure: RN is a consultant to GTx, Inc.

Abstract: Androgen receptor (AR) mediates the growth of prostate cancer (PCa) throughout its course of development, including in abnormal splice variants (AR-SV)-driven advanced stage castration-resistant disease. AR stabilization by androgens makes it distinct from other steroid receptors, which are typically ubiquitinated and degraded by proteasomes after ligand binding. Thus, targeting AR in advanced PCa requires the development of agents that can sustainably degrade variant isoforms for effective therapy. Here we report the discovery and characterization of potent selective AR degraders (SARDs) that markedly reduce the activity of wildtype and splice variant isoforms of AR at sub-micromolar doses. Three SARDs (UT-69, UT-155, and (R)-UT-155) bind the amino-terminal transcriptional activation domain AF-1, which has not been targeted for degradation previously, with two of these SARD (UT-69 and UT-155) also binding the carboxy-terminal ligand binding domain. Despite different mechanisms of action, all three SARDs degraded wild-type AR and inhibited AR function, exhibiting greater inhibitory potency than the approved AR antagonists. Collectively, our results introduce a new candidate class of next-generation therapeutics to manage advanced PCa.

Introduction: The last decade has brought several new drugs for the treatment of advanced prostate cancer (PCa). Among these are enzalutamide and apalutamide (ARN-509; NCT0231516), which are androgen receptor (AR) antagonists (1,2), as well as abiraterone, whose principal mechanism of action is to inhibit an enzyme important for androgen biosynthesis (3). Prolonged exposure of PCa cell lines and tumors to these antagonists or to conventional androgen-deprivation therapy may result in mutations in the AR ligand binding domain (LBD) or selection for cells/clones that contain these mutations and correspondingly, resistance to these molecules (4,5). PCa that relapses from medical or surgical castration and/or treatment with AR antagonists, clinically termed castration-resistant prostate cancer (CRPC), is typically lethal and effective treatment options are limited. Despite the clinical descriptor, CRPC is still dependent on the AR for its growth (6,7).

Mechanisms attributed to the development of CRPC and resistance to current treatments include over-expression of AR, expression of AR splice variants (AR-SVs) lacking the LBD, mutations in the AR in general but particularly the LBD, over-expression of coactivators and other oncogenic proteins, adrenal or intra-tumoral androgen synthesis, and activation of intracellular signaling pathways, collectively resulting in reactivation of the AR (8-14). In order to provide clinical benefit to men with CRPC with disease that is resistant to enzalutamide and/or abiraterone, next-generation AR-targeted therapeutics ideally should be able to: a) bind to any or multiple domains of the AR and inhibit its function or nuclear translocation; b) degrade the AR to prevent any inadvertent activation by any of the above mentioned alternate mechanisms; and c) inhibit the function of and degrade mutant ARs and AR-SVs.

Constitutively active and truncated AR-SVs lacking the LBD contribute to an aggressive phenotype of CRPC and render resistance to existing therapeutics (15). Recent studies have emphasized the importance of these AR-SVs in some CRPC patients. Patients with AR-V7-expressing PCa have aggressive disease with shorter progression-free- and overall- survival rates and they fail to respond to enzalutamide or abiraterone (16,17). Expression of AR-SVs is an indicator of poor prognosis (18,19). Although several studies point to the unresponsiveness of AR-SV-expressing tumors to existing treatments, other investigations have also identified a cohort of AR-SV-expressing patients responding minimally to abiraterone or enzalutamide (20). Regardless of whether these variants are drivers of resistant and/or non-resistant disease, it is important to treat such evolving forms of CRPC with drugs that also target the AR-SVs.

Here we describe first-in-class AR antagonists, UT-155 and UT-69, with unique pharmacology and chemical structure that selectively bind, inhibit, and degrade the AR and AR-SVs, including AR-V7, at nanomolar concentrations. The molecules are more potent than the reference AR antagonists tested, including enzalutamide. The advantage of such a degrader is that the reduction in AR protein prevents activation by alternate mechanisms, thereby providing a sustained treatment option for CRPC.

Materials and Methods:

Detailed methods for ChIP assay, competitive ligand binding assay, plasmid construction and transient transactivation, gene expression, Western blotting, xenograft, nuclear localization, microarray, and molecular modeling are provided in the **supplementary text**.

Reagents. Androgens, [^{3}H] mibolerone and R1881, were procured from Perkin Elmer (Waltham, MA), while lipofectamine, TaqMan PCR primers and fluorescent probes, master mixes, and Cells-

to-Ct reagents were obtained from Life Technologies (Carlsbad, CA). Dual luciferase assay reagents were purchased from Promega (Madison, WI). Dihydrotestosterone (DHT), cell culture medium, and charcoal-stripped fetal bovine serum (csFBS) were purchased from Fisher Scientific (Waltham, MA). FBS was purchased from Hyclone (San Angelo, TX). AR-N20 and AR-C19 antibodies were procured from Santa Cruz biotechnology (Santa Cruz, CA). Enzalutamide was purchased from MedKoo Biosciences (Chapel Hill, NC). Protein A sepharose was procured from GE Healthcare (Pittsburg, PA). MG-132 was purchased from R&D and bortezomib was obtained from Selleckchem (Houston, TX). All other reagents used were analytical grade. Structure and purity of enzalutamide were confirmed by NMR and mass spectrometry (**Supplemental text**).

Cell Culture. LNCaP, HEK-293, 22RV1, PC-3, and T47D cell lines were procured from the American Type Culture Collection (ATCC, Manassas, VA). All of the cells were cultured in accordance with the ATCC recommendations. The D567es and AD-1 cell lines were provided by Dr. Scott Dehm (University of Minnesota, Minneapolis, MN) (21-23) and LNCaP-abl cell line was provided by Dr. Myles Brown (Dana Farber Cancer Institute, Boston, MA) (24). The enzalutamide-resistant MR49F (LNCaP-EnzR) cell line was provided by Dr. Martin Gleave (University of British Columbia, Vancouver) (25). LNCaP-95 cells were obtained from Dr. Alan Meeker (John Hopkins Medical Institute, Baltimore, MD) (26). All cell lines were authenticated by short terminal DNA repeat assay (Genetica cell line testing laboratory, Burlington, NC).

Growth Assay. Cells were plated at varying densities and in different serum-containing medium depending on the cell line in 96-well plates, treated as indicated in the figures, and viability measured using sulforhodamine B (SRB) or cell-titer glo assay (Promega, Madison, WI).

Steady State Fluorescence Spectroscopy. Fluorescence emission spectra were measured for 1 μM AR-AF-1 as described previously (27).

Nuclear Magnetic Resonance (NMR). AF-1 and various fragments of AF-1 were cloned in pGEX4t.1 and pGEX6p.1 vectors. To purify proteins, large scale Luria broth cultures were induced with 1 mM isopropyl β-D-1-thiogalactopyranoside (IPTG) when the O.D. reached 0.6 and incubated in a shaker at 25°C for 6 hours. Cells were harvested and lysed in a lysis buffer (50 mM Tris pH 7.5, 25-250 mM NaCl, DNase, protease inhibitors, glycerol, EGTA, DTT, and sucrose). Protein lysates were purified using glutathione sepharose beads by incubating overnight at 4°C with gentle rocking and the purified protein was eluted with elution buffer (lysis buffer without DNase) containing 50 mM reduced glutathione. Purified proteins were concentrated using Amicon or GE protein concentrators. In cases where GST needed to be cleaved, precision protease was used to cleave the GST. The proteins were further purified using FPLC (GE AKTA FPLC) with gel filtration (superdex75 10/300 GL) and ion exchange (HiPrep Q FF 16/10) columns. Spectra of compounds alone or in combination with purified protein were recorded using ^{1}H NMR (Bruker 400MHz) in a total volume of 500 µl with 5 µM protein and 200-500 µM small molecule (dissolved in deuterated DMSO (d_6DMSO)) in 20 mM phosphate buffer made up in 100% deuterated water.

NMR data were collected using a Bruker AVANCE III 400MHz NMR spectrometer (Bruker BioSpin Co. Billerica, MA USA) equipped with a BBO 5 mm NMR probe, and TopSpin 3.0 software. ^{1}H proton NMR and Saturation-Transfer Difference (STD) experiments were acquired using standard pulse sequences in the TopSpin library. Spectral width was set to 16 ppm with H_2O peak at center. 32K time domain (TD) complex data points and 256 scans were used for ^{1}H proton NMR and 1024 scans for STD acquisition. For STD, on- and off-resonance were collected using interleaved method. Irradiation frequencies for on- and off-resonance were set at 0.8 ppm and -20 ppm, respectively. STD was acquired on a sample with ligand compound alone using identical settings to make sure the STD signals originated from protein in the protein-compound complex

sample. Data were collected at room temperature. Chemical shift was referenced to the H_2O peak at 4.70 ppm.

Patient specimen collection and PDX creation. Specimens from PCa patients were collected with patient consent under a protocol approved by the University of Tennessee Health Science Center (UTHSC) Institutional Review Board (IRB) in accordance to the ethical guidelines of the Declaration of Helsinki. Briefly, specimens were collected immediately after surgery in RPMI medium containing penicillin:streptomycin and fungizone and transported to the laboratory on ice. The tissues were minced finely and treated with collagenase for 2 hours. The digested tissues were washed with serum-free medium and implanted as 1 mm^3 fragments subcutaneously in Nod Scid Gamma (NSG) mice. One such PDX, Pr-3001, characterized as CRPC at the time of collection, was implanted in castrated mice. All animal studies were conducted under the UTHSC Institutional Animal Care and Use Committee (IACUC) approved protocols.

Statistics. Statistical analysis was performed using JMP-Pro (SAS Institute, Cary, NC), GraphPad prism (GraphPad Inc., La Jolla, CA), or SigmaPlot (Systat Inc., San Jose, CA) software. Experiments containing two groups were analyzed by simple t-test, while those containing more than two groups were analyzed by One Way analysis of variance (ANOVA), followed by Tukey post-hoc test.

Results: In our pursuit to develop AR degraders with nanomolar to submicromolar potency, a library of small molecules was created utilizing rational drug design based on molecular modeling of the LBD. UT-155 and UT-69 (**Figure 1A**) were selected from this focused library for more detailed *in vitro* and *in vivo* characterization and mechanistic studies. While most of the efficacy

and potency studies were performed with a dose range of 1 pM to 10 μM of the molecules, hypotheses-testing proof-of-concept mechanistic studies were performed using 10 μM.

UT-155 and UT-69 effectively antagonize the AR: All molecules in the library were tested in a battery of experiments, sequentially, to determine their binding to the LBD (using competitive radioligand binding assay) and their antagonistic activity (using transactivation assay). Molecules that bound to the AR-LBD and inhibited the AR activity were tested for their ability to decrease AR expression (using immunoblotting).

A radioligand binding assay with purified GST-AR-LBD and 1 nM ^{3}H-mibolerone showed that while UT-155 and UT-69 bound to the AR-LBD at Ki of 267 nM and 78 nM, respectively (**Figure 1A**), known antagonists such as enzalutamide, apalutamide, and galeterone bound with Ki greater than 1000 nM (**Figure 1A table**). The relative binding affinity under experimental conditions established in our laboratory indicates approximately an 8-10 fold lower Ki for UT-155 and UT-69 over enzalutamide (**Figure 1A**). The Ki for enzalutamide was weaker than previously reported in an assay using ^{18}F-FDHT as the agonist (2). While absolute Ki will differ depending on experimental conditions, the rank of relative binding affinity should remain the same.

AR transactivation assays were performed using an AR-responsive reporter and wild type AR, bicalutamide-resistant W742L, and hydroxyflutamide-resistant T878A AR mutants (28,29). UT-155 and UT-69 potently inhibited the R1881-induced wildtype AR transactivation with 6-10-fold higher potency than enzalutamide (**Figure 1B).** While UT-155 and UT-69 antagonized both

wildtype and mutant ARs comparably, enzalutamide was weaker by two fold with the W742L mutant AR relative to the wild type AR (**Figure S1A**).

To test the receptor specificity, cells were transfected as above except that expression plasmids for glucocorticoid receptor (GR), mineralocorticoid receptor (MR), and progesterone receptor (PR) and their corresponding agonists were used. Although UT-155 inhibited GR and MR transactivation, it did so only at ~10 μM (**Figure 1C**). UT-155 did however inhibit the PR transactivation at concentration comparable to that of the AR (**Figure 1C**). The same result was observed with UT-69 (data not shown).

An early event that controls AR-regulated gene expression in response to agonist is the interaction between the N-terminus and the C-terminus of the receptor (N-C interaction) (30). The N-C interaction depends on agonistic ligands, and does not occur in the presence of antagonists (30). Moreover, this N-C interaction has been shown to be important for AR interaction with chromatin (31). Given its critical role in AR function, the SARDs were tested for their ability to alter the N-C interaction using a mammalian two hybrid assay. Cells were transfected with Gal-4-DBD-AR-LBD, VP-16-AR-NTD, and Gal-4-RE-LUC, and treated with UT-69 and UT-155. Luciferase assays were performed in the cell lysates 24 hours after treatment. Both UT-155 and UT-69 significantly inhibited the AR N-C interaction with IC_{50} values comparable to that of their antagonistic IC_{50} (**Figure S1B**). Importantly, by inhibiting the N-C interaction, the SARDs will not only suppress AR transcriptional activity, but may also inhibit AR binding to chromatin.

To evaluate whether the observed highly potent AR antagonism translates to inhibition of endogenous AR function, UT-155 and UT-69 were tested in LNCaP cells and compared with enzalutamide. Treatment of LNCaP cells with UT-155 or UT-69 inhibited 0.1 nM R1881-induced PSA and FKBP5 gene expression between 10 and 100 nM with 5-10-fold better potency than enzalutamide (**Figure 1D**). We concurrently tested the effect of UT-155 on the function of enzalutamide-resistant (LNCaP-EnzR) F876L-AR (25). LNCaP-EnzR cells were treated with UT-155 or enzalutamide and the expression of PSA was measured. UT-155, but not enzalutamide, inhibited the expression of PSA in LNCaP-EnzR, indicating that the F876L mutant that is resistant to enzalutamide is sensitive to UT-155 (**Figure 1D right panel**).

UT-155 and UT-69 reduce AR expression. Our primary objective was to develop small molecules that would bind to the AR LBD and induce receptor degradation at concentrations comparable to their binding and antagonistic concentrations. We evaluated the effect of UT-155 and UT-69 on AR protein levels via Western blot using N-terminus reactive AR antibody (AR-N20). LNCaP cells were treated with UT-155 and UT-69 in the presence of 0.1 nM R1881. Both UT-155 and UT-69, but not bicalutamide, reduced the AR expression (**Figure 1E**).

Competitive antagonism is sufficient for UT-69, but not for UT-155, to inhibit AR function. UT-69 and UT-155 both compete for binding to the LBD and also reduce AR protein levels at 24 hours comparable to the observed decrease in transcriptional activity. To determine whether the reduction in expression was required to inhibit AR activity or whether the competitive displacement of androgen from the LBD is sufficient to inhibit transcriptional activity, we evaluated the effect of the SARDs on the pre-mRNA of NDRG1 and MT2A genes that are rapidly

induced by hormones (32). We hypothesized that if SARDs act exclusively by reducing AR levels, they will be unable to inhibit the induction of pre-mRNA at 1 or 2 hours as expression of AR is not reduced at this time point. Treatment of LNCaP cells with 0.1 nM R1881 increased the pre-mRNA of both NDRG1 and MT2A by 1 hour and the increase was sustained at 2 and 24 hours (**Figure 2A**). Both compounds blocked the expression of the pre-mRNA and the mRNA at 24 hours. While UT-155 failed to inhibit the R1881-dependent increase in the pre-mRNAs observed at 1 and 2 hours, UT-69 inhibited the increase even at early time points. These results indicate that while competitive antagonism through AR LBD is sufficient for the function of UT-69, degradation is necessary for UT-155. These results indicate that UT-155 is a true degrader that requires degradation to elicit its effect and competitive binding to the LBD may not have functional significance.

The distinction in the regulation of early genes between UT-69 and UT-155 provides additional information on the effect of these SARDs on AR N-C interaction. UT-155's inability to inhibit the expression of R1881-induced NDRG-1 and MT2A pre-mRNAs at 1 and 2 hours, the time points at which degradation could not be observed, suggests that UT-155 blocks the N-C interaction only as a consequence of AR degradation. On the other hand, UT-69's effect on R1881-induced NDRG1 and MT2A pre-mRNAs suggests that UT-69 may not require degradation to block the androgen-induced N-C interaction.

Enzalutamide has been reported to prevent binding of AR to chromatin. Thus we asked whether the compounds could block R1881-mediated binding to chromatin, LNCaP cells were pre-treated with UT-155 or UT-69 for 30 minutes and then with 0.1 nM R1881 for 2 hours. Two and a half

hours after the treatment, the cells were fixed to cross-link the protein to DNA. The AR was then immunoprecipitated and recruitment to the PSA enhancer was quantified by real time PCR. While UT-69 inhibited the recruitment of the AR to the ARE on the PSA enhancer, in concordance with the pre-mRNA data, UT-155 failed to inhibit the recruitment of the AR to the ARE on the PSA enhancer (**Figure 2B**). Positive control enzalutamide inhibited the recruitment of AR to PSA enhancer (**Figure 2B**). The experiments shown in the panels were performed at different times and hence the fold recruitment of AR in R1881-treated samples is somewhat different between them. Although UT-155 can compete with agonist to bind to the purified hormone binding domain (**Figure 1A**), it is possible that the enhanced stability of agonist binding in the full length receptor due to N-C interactions (33,34) is sufficient to prevent most of the binding of UT-155 to the LBD of the full length receptor.

SARDs degrade the AR: Although **Figure 1E** showed down-regulation of the AR, which likely is through enhanced degradation, there are a number of alternative possibilities including altered transcription and/or reduced translation. **Figure 3A** shows that neither compound reduces expression of AR mRNA although expression of FKBP5 is reduced as expected. **Figure 3B** shows that both compounds reduce AR expression much better than galeterone in LNCaP cells. Quantification of the blots (values expressed under the lanes) indicates that although over 50% of the receptor was degraded at 100 nM, a complete degradation could be observed at 1 μM. UT-155 also reduces AR expression in AD1 cells (**Figure 3C**).

Since the AR N-C interaction does not take place in the absence of agonist ligands, the effect of UT-69 on AR protein levels in cells grown in stripped serum was determined. As shown in **Figure**

3B, in the absence of ligands, UT-69 reduced the AR protein level below that of the level observed in vehicle-treated samples, indicating that SARD-dependent degradation of the AR does not require N-C interaction.

Selectivity of AR down-regulation was extensively tested using a range of readouts. First, the effect of UT-155 on the protein level of closely related receptors, PR and estrogen receptor (ER) was tested in T47D breast cancer cells. Although UT-155 blocked PR-dependent transactivation (**Figure 1**), it had no effect on PR or ER protein levels in T47D cells (**Figure 3D**). The effect of UT-155 on glucocorticoid receptor (GR) protein levels was tested in PC-3 cells transiently transfected with an expression construct. While UT-155 inhibited the AR protein under similar conditions, it had no effect on GR (**Figure S2A**). Second, the effect of UT-155 on the fluorescence signal emitted by GFP-AR, GFP, or GFP-ANGPTL4 (kind gift from Dr. Lawrence M. Pfeffer, University of Tennessee, TN), a protein that has no homology to nuclear receptors, was tested in HeLa cells. Treatment of HeLa cells transfected with the GFP-tagged constructs with 10 μM UT-155 resulted in down-regulation of the GFP signal in GFP-AR-transfected cells, but not in cells expressing GFP or GFP-ANGPTL4 (**Figure S2B**). Additionally, mass spectrometry was performed in LNCaP cells treated with vehicle or 10 μM UT-155. The results show that UT-155 did not inhibit the expression of the proteins identified, other than the AR. Some of the proteins identified are shown in **Figure S2C**. Finally, a study to determine the cross-reactivity of UT-155 with a panel of kinases demonstrated no significant inhibition of kinase activity. These results provide strong evidence for the selectivity of UT-155 to the AR.

To determine if the observed UT-155-dependent decrease in the AR level is due to accelerated degradation, LNCaP cells were treated with UT-155, the protein synthesis inhibitor cycloheximide, or a combination of cycloheximide and UT-155. Treatment of LNCaP cells with UT-155 decreased the AR levels by over 50% by 10 hours of treatment initiation. When LNCaP cells were treated with a combination of UT-155 and cycloheximide, a decrease in the AR protein levels was observed as early as 2-4 hours and expression was essentially lost by 6 hours (**Figure 3E**). **Figure 3E** (graph) shows the reduction in half-life of the AR by UT-155 from 10 hours to about 2 hours. Thus, the loss of protein is a result of enhanced degradation.

Phosphorylation due to altered intracellular kinase activity is an important regulator of the AR and other receptors (35,36). AR contains at least 10 phosphorylation sites, several of which have been shown to play important roles in AR function and in PCa development (35). One of the phosphorylation sites, Y^{267}, which is catalyzed by Ack1, has a known role in therapeutic resistance in CRPC (35). To determine if activation of this site would render the receptor resistant to SARD-dependent degradation, a dual approach was adopted. PC-3 cells were transfected with AR or AR in combination with a constitutively active Ack1 (CaAck1 (37); a kind gift from Dr. Shelton Earp (University of North Carolina, NC), and were treated with R1881 in the presence or absence of UT-155. UT-155 down-regulated the AR comparably in the presence or absence of CaAck1 (**Figure S3A**). In order to confirm this result, Y^{267} was mutated to aspartic acid (Y^{267D}) to provide a negative charge to this site or to phenylalanine (Y^{267F}) to block phosphorylation of this site. PC-3 cells were transfected with AR^{Y267D} or AR^{Y267F} and treated with R1881 in the presence or absence of UT-155. UT-155 down-regulated ARs carrying either of these mutants comparable to that of the wildtype AR (**Figure S3A**). This result indicates that phosphorylation at Y^{267} that confers

resistance to therapeutics does not alter the ability of UT-155 to degrade the AR and might provide some supporting evidence for our hypothesis that degrading the AR will potentially overcome therapeutic resistance.

UT-155 promotes degradation potentially through proteasome pathway. In order to test the mechanism of degradation, LNCaP cells were treated with UT-155 in the presence of the proteasome inhibitor, bortezomib. Earlier studies have demonstrated that MG-132 inhibits AR protein and AR transactivation and blocks AR nuclear translocation (38). This effect was observed clearly in cells treated with UT-155 and MG-132 (**Figure 3F**). To overcome this confounding effect on AR expression and localization by MG-132, a clinically used proteasome inhibitor, bortezomib (Velcade), was used to determine the role of proteasome pathway in UT-155's effect on AR stability. Earlier studies with bortezomib have not reported any significant effect on AR expression or function (39). UT-155 down-regulated the AR protein by 40% in LNCaP cells treated for 9 hours. This reduction in AR protein was reversed by bortezomib to the level observed in R1881-treated cells (**Figure 3F**). This result indicates that UT-155 potentially down-regulates the AR through the proteasome pathway. To determine the consequence of proteasome inhibition on UT-155's inhibitory effect on AR transactivation, HEK-293 cells were transfected with GRE-LUC, AR, and CMV-renilla-LUC plasmids and the cells were treated with UT-155 alone or in combination with bortezomib in the presence of R1881. UT-155 inhibited the AR transactivation induced by 0.1 nM R1881, and this complete inhibition was partially reversed by bortezomib (**Figure S3B**). These results indicate the potential role of the proteasome pathway in UT-155-dependent AR degradation and functional inhibition.

UT-155 promotes degradation of splice-variants of AR. To confirm the capacity of UT-155 to induce degradation of AR in different cell lines, we studied the effects of UT-155 in 22RV1 cells, which express AR and an AR-SV, AR-V7 (26,40). 22RV1 cells were treated with a dose response of UT-155 in charcoal-stripped serum (CSS)-containing medium to represent an androgen-independent state. UT-155 treatment resulted in the degradation of the AR in 22RV1 cells (**Figure 4A**). Remarkably and unexpectedly, UT-155 also degraded AR-V7 in the same experiment.

To validate the results obtained in 22RV1 cells and to ensure that these effects are not cell line specific, the ability of UT-155 to promote degradation of the AR-SV was tested in multiple PCa cell lines. D567es cells that express AR-SV, AR-v567es, and LNCaP-95 cells that express AR-FL and AR-SV were treated with a dose range of UT-155. The cells were harvested 24 hours after treatment and a Western blot for the AR and its isoforms was performed (**Figure 4A**). UT-155 consistently led to degradation of the AR and its SVs at concentrations ranging between 100 and 1000 nM, indicating that these SARDs promote degradation of the AR and its SVs under various conditions and regardless of the permutation-combination of the AR-FL and SV expression. The D567es result suggests a direct interaction of the molecule with the AR-SV. Since the LNCaP-95 blot was over-exposed to show the effect on AR-SV, which is minimally expressed in this cell line, the experiment was repeated with lower protein concentration loaded on to the gel to visualize the degradation of the AR-full length (**Figure 4A**).

We also repeated the experiment shown in **Figure 3E** in 22RV1 cells to confirm that AR-SV down-regulation induced by UT-155 was a result of decreased protein stability. Similar to the experimental conditions in LNCaP cells, the 22RV1 cells were treated with UT-155,

cycloheximide, or a combination of UT-155 and cycloheximide and the expression of the AR and the AR-SV was determined. UT-155 and cycloheximide each decreased the levels of both the AR and the AR-SV and degradation was accelerated in the combination treatment (**Figure 4B**).

Since UT-155 down-regulated the AR-SV protein expressed in various PCa cell lines, we performed experiments to determine the effect of UT-155 on the transcriptional activity of two constitutively active AR variants, the clinically relevant AR-V7 and a synthetic construct lacking the LBD (AR A/BCD). Transactivation assays demonstrated that the activity of AR A/BCD (**Figure S4A left**) was significantly inhibited by UT-155 (**Figure S4A right)**, but not by enzalutamide. Similarly, AR-V7-induced transactivation of a UBE2C-promoter luciferase construct (kind gift from Dr. Yan Dong, Tulane University (41)) was significantly inhibited by UT-155, but not by enzalutamide (**Figure S4B**). These results suggest that down-regulation of AR-SVs has significant functional consequences.

Interestingly, AR and AR-SV nuclear localization experiments with UT-155 in enzalutamide-resistant LNCaP and D567es cells, respectively show that UT-155 inhibits nuclear localization of the AR and AR v567es (**Figure S5A and S5B**), indicating that these molecules have multifaceted properties of both degradation and inhibition of nuclear localization. Although v567es in D567es cells is localized both in the cytoplasm and in the nucleus, the nuclear localization was reduced and the punctate foci observed in the nuclei were reduced significantly in UT-155 treated cells.

UT-155 inhibits AR-SV-dependent gene expression. The effect of UT-155 on AR-V7-dependent gene expression was determined in 22RV1 cells. 22RV1 cells plated in charcoal stripped serum-

containing medium were treated with vehicle or 10 μM UT-155 for 48 hours and the expression of FKBP5 was measured and normalized to GAPDH. The effect on AR-V7-dependent FKBP5 expression was inhibited by UT-155, but not by enzalutamide (**Figure 4C**).

SARDs bind to the AR-AF-1 domain. As UT-155 selectively promotes degradation of the AR-SVs without the need for either AR-FL or other partner proteins (cycloheximide experiment), we speculated that in addition to its binding to the AR-LBD, UT-155 binds to a region in the N-terminal domain (NTD). However, the NTD is known to be an intrinsically disordered region of the AR with a dearth of reported small molecule ligands, complicating the development of a standard competitive binding assay (42,43). Consequently, we sought to demonstrate binding via biophysical analyses of ligand in the presence and absence of various AF-1 derived peptides. Previous studies have shown that molecules that bind to the NTD region are associated with the AF-1 domain that resides between amino acids 141-486 in the NTD region (27).

As a first-step, we evaluated the binding of UT-155 to AF-1 (amino acids 141-486) using steady-state fluorescence emission spectroscopy. There are two tryptophan residues and up to 12 tyrosine residues in the AF-1 domain, providing an opportunity to study the folding properties of this domain using intrinsic steady-state fluorescence emission spectra. Excitation at 287 nm excites both tyrosine and tryptophan residues (44). This method has been validated as a small molecule binding assay and was used to determine binding of small molecules to human serum albumin (45) and proteins in saliva (46). To measure the interaction of the individual compounds, steady-state fluorescence was measured in the presence of a dose response of UT-155 and the AF-1 protein.

UT-155 bound to the AR AF-1 with a Kd of 1.32 μM (**Figure 5A**). These results were reproduced with UT-69 (**Figure S6A**).

To confirm the results obtained through the fluorescence emission spectra, we employed the Biacore method using biotin-labeled AF-1 purified protein. The Biacore assay uses surface plasmon resonance (SPR) to measure protein-protein and protein-small molecule interactions (47). In this assay, AR AF-1 and 50 nM of UT-155 (**Figure S6B left)** or UT-69 (**Figure S6B right**) were added to a Biacore chip and SPR was measured. The red and the green lines correspond to reference biosensors, while the blue lines are the AF-1-loaded biosensors. As can be clearly seen, while UT-155 and UT-69 had no effect on the reference biosensors-loaded chips, UT-155 and UT-69 shifted the spectra when the chips were loaded with the AF-1 protein. These results confirm the interaction of UT-155 and UT-69 with AF-1 as measured by a change in the refraction index in the SPR (**Figure S6B**).

NMR studies confirm the binding of UT-155 to AF-1 between amino acids 244-360. ^{1}H NMR has been used in high-throughput screens to detect the binding of small molecules less than 500 Da to large proteins greater than 5 KDa (48,49). As opposed to other biophysical methods, it is easier to use one dimension NMR to observe changes in line-width or line broadening as a high-throughput method to identify the binding of the molecules to proteins and then use Water ligand-observed spectroscopy (WaterLOGSY) or Saturation-Transfer Difference (STD) NMR as confirmatory methodologies (50). These experiments are based on the fact that NMR observables such as linewidths and NOEs vary dramatically between small molecules and large molecules. The decreased rotational correlation times upon binding of a small molecule ligand to a heavy target

molecule produces an atypical heavy molecule NMR result characterized by broadening and weakening of ligand peaks in ^{1}H NMR and negative NOE peaks in the WaterLOGSY as compared to the free state. In the absence of any affinity, the small molecule NMR result is obtained (sharp peaks in ^{1}H NMR and positive NOEs). This distinction provides the basis for NMR screening experiments.

Using these principles, ^{1}H NMR was utilized to confirm the binding of UT-155 to the AF-1 region. In the first experiment, UT-155 or enzalutamide (500 μM) was dissolved in deuterated D_6DMSO and was incubated alone or mixed with 5 μM GST-AF-1 or GST and the binding of the molecules to the protein was determined by NMR. While UT-155 alone or in combination with GST exhibited sharp peaks revealing the ligand present in the free state, UT-155 in combination with GST-AF-1 provided broad, diffused, and shorter ligand peaks (**Figure 5B;** peaks in box) revealing that UT-155 has affinity for AF-1. Alternatively, the negative control enzalutamide known to bind to the LBD failed to exhibit a shorter and broader peak in the presence of AF-1 revealing no affinity for AF-1. This result confirms that the UT-155, but not enzalutamide, binds to the AF-1 domain. To further confirm the NMR results, we performed WaterLOGSY with UT-155 alone or in combination with AF-1. While the UT-155 alone gave a flat signal, UT-155 in combination with AF-1 provided a negative signal, characteristic of binding to the protein (**Figure 5C**).

To determine the precise location within the AF-1 region where UT-155 binds (since the AF-1 region is between 141 and 486 amino acids), smaller fragments of AF-1 were produced and purified (**Figure 5D**). UT-155 was incubated alone or in combination with GST, GST-AF-1 or with the various fragments of the AF-1 region and ^{1}H NMR profiles were obtained. Similar to the

results shown in **Figure 5B,** UT-155 provided a sharp signal by itself and when co-incubated with GST, but provided a broad shorter peak when incubated with AF-1 (**Figure 5E**). Similar to the unbound ligand, UT-155 in combination with fragments 1A and 5T gave sharp, tall peaks. However, when UT-155 was incubated with fragment 1T, the signal was almost indistinguishable from baseline, indicating binding affinity to this region. The profile of UT-155 in combination with 1B looked similar to that of the AF-1 profile, confirming a binding to this region. Binding of UT-155 to 1T and 1B, but not to 1A, indicates that amino acids 51-211 could be excluded and that the binding occurs between amino acids 244 and 360.

Three separate biophysical methods, fluorescence spectra, SPR, and NMR indicate that UT-155 (and UT-69) have significant affinity for AF-1, suggestive of binding strong enough to mediate some of the unique characteristics of the AR antagonists reported herein.

STD-NMR has been used to determine the binding/interaction of a ligand to a receptor. It is based on the nuclear Overhauser effect and the principle is based on the ligand resonance signal. An STD confirmatory experiment with purified GST-cleaved 1T and UT-155 showed that while the UT-155 alone had no peaks, UT-155 when combined with 1T showed the peaks corresponding to UT-155 (**Figure S6C**). The STD-NMR result served as confirmation for the binding of UT-155 to the 1T region.

Identification of a SARD that binds to the AF-1, but not to the LBD. The SARDs described here have multiple properties. Although UT-155 binds to the isolated LBD, the studies described so far demonstrated that degradation is required for UT-155-mediated inhibition of AR activity. To

determine the domain that is important for UT-155's function, we utilized multiple experimental approaches, including site-directed mutagenesis and synthesis of (*R*)-UT-155.

Molecular modeling was performed to determine the amino acids in the AR-LBD with which UT-155 interacted. UT-155 forms hydrogen bonds with Q711, R752, N705, and L704 (**Figure 6A**). These sites were mutated and a transactivation assay was performed. Mutating these amino acids individually compromised the ability of R1881 to activate the AR. While the EC_{50} of R1881 for the wildtype AR was 0.11 nM, the EC_{50} for the mutant ARs was 7.48 nM for Q711A, 8.72 nM for L704A, 15.41 nM for R752L, and 2037 nM for N705A (**Figure 6A**). Effect of UT-155 on the AR mutants transactivation in the presence of 10 nM R1881 was evaluated. The results demonstrated that mutating the interacting amino acid residues failed to weaken the antagonistic profile of UT-155 (**Figure 6A**). This indicates that although UT-155 interacts with these amino acids, they are not critical for its function, which is in concordance with the results obtained with the pre-mRNAs (**Figure 2A**).

UT-155 has a chiral center and the active form at the AR LBD is the S-isomer. We synthesized an *R*-isomer (UT-123 or (R)-UT-155), which is expected to be a weaker LBD binder than the S-isomer. Radioligand binding assay showed that while the S- isomer bound to the AR LBD with a Ki of 267 nM, the *R*-isomer failed to bind to the AR LBD until 10,000 nM (**Figure 6B**). We tested the effect of (*R*)-UT-155 on R1881-induced AR transactivation and AR expression. The (*R*)-UT-155 was comparable to the (*S*)-UT-155 in inhibiting AR transactivation and degrading the AR with only marginal weakening observed in the antagonistic effect (**Figure 6B**). (*R*)-UT-155 also inhibited the AR N-C interaction (**Figure S1B**). These results show that binding to the LBD is not

needed for the antagonistic and degradation effects of UT-155. Since (*R*)-UT-155 failed to bind to the LBD yet retained its capacity to induce degradation resulting in loss of activity, we speculated that it exclusively binds to the AF-1 domain. We performed an NMR experiment to determine its binding to the AF-1. As expected (*R*)-UT-155 bound to the AF-1 domain (**Figure 6C**), making it the first known AF-1 binding degrader. Further, the effect of (*R*)-UT-155 on LNCaP cell growth and AR-target gene expression was determined. (*R*)-UT-155 inhibited the proliferation of LNCaP cells and the R1881-induced expression of AR-target gene, FKBP5 at concentrations comparable to that observed with UT-155 (**Figure 6D**).

SARDs alter LNCaP transcriptome more potently than enzalutamide: Since the SARDs not only antagonize the AR, like enzalutamide, but also degrade the AR, the SARDs might affect the transcriptome more robustly than enzalutamide. To test this hypothesis, a microarray study was performed in LNCaP cells maintained in charcoal-stripped serum-containing medium for 2 days and treated with 10 μM of enzalutamide, UT-155, (*R*)-UT-155, and UT-69 in the presence of 0.1 nM R1881 for 24 hours. The results, based on a cut-off of 2-fold change from vehicle-treated samples, indicate that UT-155, UT-69, and (*R*)-UT-155 altered the expression of approximately 3000 genes, while enzalutamide altered the expression of 927 genes (**Figure S7A**). The differential regulation of gene expression could be due to the weaker response elicited by enzalutamide. A similar number of genes were up- and down- regulated by all the molecules. Several AR-regulated genes such as KLK3 (PSA), TMPRSS2, NKx3.1 and others were down-regulated in the drug-treated samples. Although an overlap of about 300 genes between SARDs and enzalutamide samples could be observed, the SARDs altered the genes robustly than enzalutamide (**Figure S7B**). The highest change in SARD-treated samples was between 350- and 550- fold, while that in

enzalutamide-treated samples was only 22-fold. This suggests that the SARDs may be more powerful modifiers of AR function than enzalutamide. Ten genes from the microarray dataset were validated by real-time PCR. The results of the real-time PCR validation are in concordance with the microarray data (**Figure S7C**). The gene that was maximally induced by all the SARDs is a cellular stress-response transcription factor, activation transcription factor-3 (ATF-3) (51).

The expression data was analyzed using String software (https://string-db.org/). The top canonical pathways enriched by the genes regulated by the SARDs and enzalutamide are cellular responses to chemical stimuli and stress-related pathways.

UT-155 inhibits AR- and AR-SV -dependent PCa cell proliferation. To determine whether the degradation and inhibition of the AR function translates into PCa cell growth inhibition, the effect of SARDs on the proliferation of AR-dependent LNCaP, LNCaP-abl, and LNCaP-EnzR cells was tested. R1881-induced LNCaP proliferation was completely inhibited by UT-155 in hundreds of nanomolar concentration, while enzalutamide inhibited the proliferation at concentrations greater than 1 μM (**Figure 7A**). These results were reproduced in various cell lines, including LNCaP-abl, whose growth is androgen independent and resistant to AR antagonists, and in LNCaP-EnzR (**Figure 7A**). UT-155 only modestly inhibited the proliferation of HeLa cells at 30 μM, demonstrating its specificity for AR-expressing cells (**Figure 7A**).

To determine whether the inhibition of the AR-SV function translates into PCa cell growth inhibition, the effect of SARDs on the proliferation of AR-FL- and AR-SV-expressing cell lines was evaluated. UT-155 inhibited the proliferation of 22RV1 cells at concentrations between 1 and

10 μM, while enzalutamide failed to inhibit the proliferation (**Figure 7B**). These results were reproduced in another AR-SV-expressing cell line, LNCaP-95 that expresses AR and AR-SV (**Figure 7B**). The AR-SV transactivation results shown in **Figure S4** and the proliferation results observed in **Figure 7B** were also reproduced in R1-D567es cells, where UT-155 inhibited the transactivation of v567es and the proliferation of D567es cells (**Figure S8B**). We also tested the SARDs for their ability to inhibit the growth of an AR-negative PCa cell line, PC-3. Although the SARDs degrade the ectopically-expressed AR in PC-3 cells, indicating the availability of the machinery for AR degradation, the SARDs failed to inhibit the proliferation of PC-3, growth of which is not dependent on AR, after 6 days of treatment (**Figure S8C**), further confirming their specificity. A comparison between the LNCaP and PC-3 cell growth in the presence of UT-155 is provided in the **right panel**.

UT-155 inhibits growth of PCa xenografts. The studies described above *in vitro* models provide support that UT-155 inhibits and promotes degradation of both AR-FL and mutant AR. To determine the effects *in vivo*, UT-155 was tested in xenograft models. Because the metabolic properties of UT-155 were 5-10 fold better than that of UT-69 and that the half-life of UT-69 in liver microsomes was not optimal for *in vivo* testing (**Figure S8D and S8F**), we performed *in vivo* studies with UT-155 and not with UT-69. UT-155 inhibited the growth of the LNCaP tumors with a 65% tumor growth inhibition (TGI) (**Figure 7C**). Consistent with the inhibition of tumor volume, tumor weights and tumor PSA were also significantly lower by 50-75% in UT-155-treated animals (**Figure 7C**).

UT-155 inhibits growth of AR-SV-dependent prostate cancer xenografts. Consistent with the anti-proliferative effects *in vitro*, UT-155 significantly inhibited the growth of 22RV1 xenograft by 53%, while, as expected, enzalutamide had no effect on the growth of the 22RV1 tumors (**Figure 7D**). Tumor weights and PSA and the expression of AR and AR-SV were significantly lower in UT-155-treated animals (**Figure 7D**).

In the measurement of drug concentration in the tumors to determine the drug exposure, UT-155 was extracted from tumors and was detected by mass spectrometry. UT-155 accumulated in the tumors and the concentration of 562 nM was above its IC_{50} concentration (**Figure S8F**).

Pr-3001 is a patient-derived xenograft (PDX) developed using a specimen from an aggressively growing metastatic prostate cancer with Gleason score 10 (5+5). Pr-3001 develops tumors robustly and attains approximately 1000 mm^3 in less than 2 months. Pr-3001 expresses AR-FL and AR-SV and grows in castrated mice. Pr-3001 as a 1 mm^3 piece was implanted on the flanks of mice and its growth was monitored. When Pr-3001 attained 100-200 mm^3, the animals were randomized and treated with vehicle or UT-155. Consistent with the observations made in 22RV1 xenografts, UT-155 inhibited the growth of Pr-3001 by 40-60% over the course of 14 days (**Figure 7E**).

Discussion: Using hormone binding, transactivation assays, and Western blotting, we sought to identify AR antagonists that induced degradation of AR. Based on our preliminary data, we further characterized two compounds, UT-69 and UT-155. These studies yielded some surprising results. Whereas UT-69 apparently competes with agonist binding to immediately block transcription with a longer term effect of virtually eliminating expression through enhanced degradation, UT-155

displays distinct properties. Although UT-155 competes for binding of agonist when measured using a purified LBD, it fails to block the initial induction of transcription (**Figure 2**). This is not due to intrinsic agonist activity of the compound because treatment with UT-155 alone yields activity comparable to UT-69 alone (**Figure 2A, 1 hour**). The pre-mRNA data suggest that UT-155 may not bind to the LBD in native full-length conformation or may bind transiently enough (faster off-rate) to not have an impact. The agonist-induced N-C interaction is known to slow the off-rate of agonists (33). However, similar to UT-69, UT-155 induces degradation of AR, and thus at 24 hours AR activity is eliminated. Remarkably, these compounds inhibit activity and cause degradation not only of AR and its point mutants, but also induce degradation of AR-SVs. This finding raised the question of whether the compounds also bound to the NTD since the AR-SVs lack the LBD.

Due to the lack of a radioligand competitive binding assay, we acknowledge that the bar to demonstrate the binding to AF-1 is much higher. Hence, we used multiple independent biophysical methods including fluorescence polarization assay, Biacore SPR, and NMR using the AF-1 domain purified proteins. We also used molecular analytical methods such as Western blots that measure the degradation of the AR-SVs that lack LBD, in order to demonstrate the interaction with AF-1. All assays demonstrated a direct interaction, although the concentrations of components needed to detect an interaction differed due to technical limitations and the sensitivities of the techniques.

That binding to the AF-1 promotes the degradation is supported by the sensitivity of the AR-SVs to the compounds as well as the finding that (*R*)-UT-155, which binds only to the AF-1 domain,

also induces degradation. Moreover, although UT-155 inhibits PR activity presumably by binding to the LBD (**Figure 1**), it does not induce degradation (**Figure 3D**) supporting specificity of the compounds.

Interest in targeting the NTD or DNA binding of AR has increased since the discovery of the AR-SVs. Due to the intrinsically disorganized nature of the AR-NTD, its structure has not been resolved, making it difficult to develop drugs targeting this domain (52). Any drug that is developed for the NTD has to be developed either by screening a large library (27) or by serendipity as in our case. EPI-001 and EPI-002, discovered using high-throughput screening have been shown to bind to the AR-NTD and inhibit AR function (27). Despite its low affinity interaction with the AR-NTD, EPI-001 may have other activities that contribute to its biological efficacy, including destabilization of AR mRNA or through peroxisome proliferator and activated receptor gamma (PPAR-ɣ) cross-reactivity (53). Another molecule described as being an AR degrader is ASC-J9, *albeit* its direct binding to the AR has not yet been demonstrated and it induces degradation at concentrations greater than 10 μM.

Although UT-69 inhibited AR activity directly by inducing degradation, UT-155 was equally efficacious at 24 hours and was chosen for the *in vivo* studies due to its better pharmacokinetic (PK) properties. UT-155 reduced growth of tumors in three prostate cancer models (**Figure 7**) and the partial reduction of AR in the 22RV1 tumors suggests that optimization of the compound, leading to more extensive reduction in AR would improve efficacy.

It should be noted that although UT-155 is more potent than enzalutamide by a log unit *in vitro*, it has to be administered at a much higher dose *in vivo* than enzalutamide (**Figure 7D**). UT-155 is a first-generation molecule in our library with sub-optimal PK properties. Lead optimization is currently being performed to obtain molecules with optimum PK properties, while retaining the desired degradation properties. Secondly, enzalutamide's poor solubility precluded the use of a dose comparable to that of UT-155. While degradation and AF-1 binding will be the primary and secondary lead optimization criteria, importance will also be given to obtaining an orally bioavailable drug with an optimum PK profile.

The salient features of the SARDs have the potential to provide an AR-targeted therapeutic approach for patients who have developed enzalutamide-resistant cancers. In addition, degradation of the AR and AR-SV will prevent activation by IL-6, PKA, coactivators, intra-tumoral androgens, and others. The AR AF-1 domain is the primary domain responsible for coactivator interaction (54). Molecules such as UT-155 and UT-69 that bind to the AF-1 domain could confer advantages by blocking the AR interaction with coactivators, which is essential for AR function. Considering that the AF-1 is the functionally important domain, binding of the SARDs to the LBD is not as important as the degradation of the AR and AR-SVs. Leads will be optimized based on the selective degradation of the AR and AR-SV obtained by binding to the AF-1 domain. If binding to the LBD is imperative to inhibit prostate cancer completely, these SARDs could be combined with enzalutamide or other LBD-binding antagonists.

There is an urgent need to develop novel therapeutic approaches for men with advanced prostate cancer that are not responsive or become resistant to currently used agents. Rapid and sustained

degradation of the AR and AR-SV with a novel mechanism of action suggests that these SARDs may provide for such an approach.

Acknowledgements: The authors thank Mr. Maron Lee Barrett and Ms. Mayra Star for their technical help. The authors thank Dr. Dejian Ma for his technical help with the NMR studies. The authors thank the UTHSC and St. Jude NMR core for their help with the NMR studies. The authors thank Drs. Robert Getzenberg and Michael Mohler for providing useful comments on the manuscript. The authors thank Ms. Brandy Grimes for her help with tissue procurement. The authors thank Dr. Daniel Johnson of UT BioCore for microarray data analysis and Mr. Lorne Rose of UT-MRC core for microarray studies.

References:

1. Clegg NJ, Wongvipat J, Joseph JD, Tran C, Ouk S, Dilhas A, *et al.* ARN-509: a novel antiandrogen for prostate cancer treatment. Cancer research **2012**;72:1494-503
2. Tran C, Ouk S, Clegg NJ, Chen Y, Watson PA, Arora V, *et al.* Development of a second-generation antiandrogen for treatment of advanced prostate cancer. Science **2009**;324:787-90
3. Attard G, Reid AH, A'Hern R, Parker C, Oommen NB, Folkerd E, *et al.* Selective inhibition of CYP17 with abiraterone acetate is highly active in the treatment of castration-resistant prostate cancer. J Clin Oncol **2009**;27:3742-8
4. Joseph JD, Lu N, Qian J, Sensintaffar J, Shao G, Brigham D, *et al.* A clinically relevant androgen receptor mutation confers resistance to second-generation antiandrogens enzalutamide and ARN-509. Cancer Discov **2013**;3:1020-9
5. Bohl CE, Gao W, Miller DD, Bell CE, Dalton JT. Structural basis for antagonism and resistance of bicalutamide in prostate cancer. Proceedings of the National Academy of Sciences of the United States of America **2005**;102:6201-6
6. Schalken J, Fitzpatrick JM. Enzalutamide: Targeting the androgen signalling pathway in metastatic castration-resistant prostate cancer. BJU international **2015**
7. Scher HI, Buchanan G, Gerald W, Butler LM, Tilley WD. Targeting the androgen receptor: improving outcomes for castration-resistant prostate cancer. Endocrine-related cancer **2004**;11:459-76

8. Chism DD, De Silva D, Whang YE. Mechanisms of acquired resistance to androgen receptor targeting drugs in castration-resistant prostate cancer. Expert review of anticancer therapy **2014**;14:1369-78
9. Nazareth LV, Weigel NL. Activation of the human androgen receptor through a protein kinase A signaling pathway. The Journal of biological chemistry **1996**;271:19900-7
10. Sadar MD, Gleave ME. Ligand-independent activation of the androgen receptor by the differentiation agent butyrate in human prostate cancer cells. Cancer research **2000**;60:5825-31
11. Sadar MD. Androgen-independent induction of prostate-specific antigen gene expression via cross-talk between the androgen receptor and protein kinase A signal transduction pathways. The Journal of biological chemistry **1999**;274:7777-83
12. Agoulnik IU, Vaid A, Nakka M, Alvarado M, Bingman WE, 3rd, Erdem H, *et al.* Androgens modulate expression of transcription intermediary factor 2, an androgen receptor coactivator whose expression level correlates with early biochemical recurrence in prostate cancer. Cancer research **2006**;66:10594-602
13. Labrie F. Blockade of testicular and adrenal androgens in prostate cancer treatment. Nature reviews Urology **2011**;8:73-85
14. Shafi AA, Yen AE, Weigel NL. Androgen receptors in hormone-dependent and castration-resistant prostate cancer. Pharmacol Ther **2013**;140:223-38
15. Lu J, Van der Steen T, Tindall DJ. Are androgen receptor variants a substitute for the full-length receptor? Nature reviews Urology **2015**;12:137-44
16. Antonarakis ES, Lu C, Wang H, Luber B, Nakazawa M, Roeser JC, *et al.* AR-V7 and resistance to enzalutamide and abiraterone in prostate cancer. The New England journal of medicine **2014**;371:1028-38
17. Scher HI, Lu D, Schreiber NA, Louw J, Graf RP, Vargas HA, *et al.* Association of AR-V7 on Circulating Tumor Cells as a Treatment-Specific Biomarker With Outcomes and Survival in Castration-Resistant Prostate Cancer. JAMA Oncol **2016**
18. Hornberg E, Ylitalo EB, Crnalic S, Antti H, Stattin P, Widmark A, *et al.* Expression of androgen receptor splice variants in prostate cancer bone metastases is associated with castration-resistance and short survival. PloS one **2011**;6:e19059
19. Kong D, Sethi S, Li Y, Chen W, Sakr WA, Heath E, *et al.* Androgen receptor splice variants contribute to prostate cancer aggressiveness through induction of EMT and expression of stem cell marker genes. The Prostate **2015**;75:161-74
20. Bernemann C, Schnoeller TJ, Luedeke M, Steinestel K, Boegemann M, Schrader AJ, *et al.* Expression of AR-V7 in Circulating Tumour Cells Does Not Preclude Response to Next Generation Androgen Deprivation Therapy in Patients with Castration Resistant Prostate Cancer. Eur Urol **2016**
21. Chan SC, Selth LA, Li Y, Nyquist MD, Miao L, Bradner JE, *et al.* Targeting chromatin binding regulation of constitutively active AR variants to overcome prostate cancer resistance to endocrine-based therapies. Nucleic Acids Res **2015**;43:5880-97
22. Li Y, Chan SC, Brand LJ, Hwang TH, Silverstein KA, Dehm SM. Androgen receptor splice variants mediate enzalutamide resistance in castration-resistant prostate cancer cell lines. Cancer research **2013**;73:483-9
23. Nyquist MD, Li Y, Hwang TH, Manlove LS, Vessella RL, Silverstein KA, *et al.* TALEN-engineered AR gene rearrangements reveal endocrine uncoupling of androgen receptor in

prostate cancer. Proceedings of the National Academy of Sciences of the United States of America **2013**;110:17492-7
24. Culig Z, Hoffmann J, Erdel M, Eder IE, Hobisch A, Hittmair A, *et al.* Switch from antagonist to agonist of the androgen receptor bicalutamide is associated with prostate tumour progression in a new model system. Br J Cancer **1999**;81:242-51
25. Kuruma H, Matsumoto H, Shiota M, Bishop J, Lamoureux F, Thomas C, *et al.* A novel antiandrogen, Compound 30, suppresses castration-resistant and MDV3100-resistant prostate cancer growth in vitro and in vivo. Mol Cancer Ther **2013**;12:567-76
26. Hu R, Dunn TA, Wei S, Isharwal S, Veltri RW, Humphreys E, *et al.* Ligand-independent androgen receptor variants derived from splicing of cryptic exons signify hormone-refractory prostate cancer. Cancer research **2009**;69:16-22
27. Andersen RJ, Mawji NR, Wang J, Wang G, Haile S, Myung JK, *et al.* Regression of castrate-recurrent prostate cancer by a small-molecule inhibitor of the amino-terminus domain of the androgen receptor. Cancer Cell **2010**;17:535-46
28. Hara T, Miyazaki J, Araki H, Yamaoka M, Kanzaki N, Kusaka M, *et al.* Novel mutations of androgen receptor: a possible mechanism of bicalutamide withdrawal syndrome. Cancer research **2003**;63:149-53
29. Tan J, Sharief Y, Hamil KG, Gregory CW, Zang DY, Sar M, *et al.* Dehydroepiandrosterone activates mutant androgen receptors expressed in the androgen-dependent human prostate cancer xenograft CWR22 and LNCaP cells. Mol Endocrinol **1997**;11:450-9
30. He B, Lee LW, Minges JT, Wilson EM. Dependence of selective gene activation on the androgen receptor NH2- and COOH-terminal interaction. The Journal of biological chemistry **2002**;277:25631-9
31. Li J, Fu J, Toumazou C, Yoon HG, Wong J. A role of the amino-terminal (N) and carboxyl-terminal (C) interaction in binding of androgen receptor to chromatin. Mol Endocrinol **2006**;20:776-85
32. Trevino LS, Bolt MJ, Grimm SL, Edwards DP, Mancini MA, Weigel NL. Differential Regulation of Progesterone Receptor-Mediated Transcription by CDK2 and DNA-PK. Mol Endocrinol **2016**;30:158-72
33. He B, Kemppainen JA, Voegel JJ, Gronemeyer H, Wilson EM. Activation function 2 in the human androgen receptor ligand binding domain mediates interdomain communication with the NH(2)-terminal domain. The Journal of biological chemistry **1999**;274:37219-25
34. Doesburg P, Kuil CW, Berrevoets CA, Steketee K, Faber PW, Mulder E, *et al.* Functional in vivo interaction between the amino-terminal, transactivation domain and the ligand binding domain of the androgen receptor. Biochemistry **1997**;36:1052-64
35. Mahajan K, Coppola D, Rawal B, Chen YA, Lawrence HR, Engelman RW, *et al.* Ack1-mediated androgen receptor phosphorylation modulates radiation resistance in castration-resistant prostate cancer. The Journal of biological chemistry **2012**;287:22112-22
36. Narayanan R, Adigun AA, Edwards DP, Weigel NL. Cyclin-dependent kinase activity is required for progesterone receptor function: novel role for cyclin A/Cdk2 as a progesterone receptor coactivator. Mol Cell Biol **2005**;25:264-77
37. Mahajan NP, Whang YE, Mohler JL, Earp HS. Activated tyrosine kinase Ack1 promotes prostate tumorigenesis: role of Ack1 in polyubiquitination of tumor suppressor Wwox. Cancer research **2005**;65:10514-23
38. Lin HK, Altuwaijri S, Lin WJ, Kan PY, Collins LL, Chang C. Proteasome activity is required for androgen receptor transcriptional activity via regulation of androgen receptor

nuclear translocation and interaction with coregulators in prostate cancer cells. The Journal of biological chemistry **2002**;277:36570-6

39. Ikezoe T, Yang Y, Saito T, Koeffler HP, Taguchi H. Proteasome inhibitor PS-341 down-regulates prostate-specific antigen (PSA) and induces growth arrest and apoptosis of androgen-dependent human prostate cancer LNCaP cells. Cancer Sci **2004**;95:271-5
40. Guo Z, Yang X, Sun F, Jiang R, Linn DE, Chen H, *et al.* A novel androgen receptor splice variant is up-regulated during prostate cancer progression and promotes androgen depletion-resistant growth. Cancer research **2009**;69:2305-13
41. Zhan Y, Zhang G, Wang X, Qi Y, Bai S, Li D, *et al.* Interplay between Cytoplasmic and Nuclear Androgen Receptor Splice Variants Mediates Castration Resistance. Mol Cancer Res **2017**;15:59-68
42. Monaghan AE, McEwan IJ. A sting in the tail: the N-terminal domain of the androgen receptor as a drug target. Asian J Androl **2016**;18:687-94
43. McEwan IJ. What lies beneath: natural products from marine organisms as nuclear receptor modulators. Biochem J **2012**;446:e1-3
44. Reid J, Murray I, Watt K, Betney R, McEwan IJ. The androgen receptor interacts with multiple regions of the large subunit of general transcription factor TFIIF. The Journal of biological chemistry **2002**;277:41247-53
45. Epps DE, Raub TJ, Caiolfa V, Chiari A, Zamai M. Determination of the affinity of drugs toward serum albumin by measurement of the quenching of the intrinsic tryptophan fluorescence of the protein. J Pharm Pharmacol **1999**;51:41-8
46. Rawel HM, Frey SK, Meidtner K, Kroll J, Schweigert FJ. Determining the binding affinities of phenolic compounds to proteins by quenching of the intrinsic tryptophan fluorescence. Mol Nutr Food Res **2006**;50:705-13
47. Rich RL, Myszka DG. BIACORE J: a new platform for routine biomolecular interaction analysis. J Mol Recognit **2001**;14:223-8
48. Shortridge MD, Hage DS, Harbison GS, Powers R. Estimating protein-ligand binding affinity using high-throughput screening by NMR. J Comb Chem **2008**;10:948-58
49. Dias DM, Ciulli A. NMR approaches in structure-based lead discovery: recent developments and new frontiers for targeting multi-protein complexes. Prog Biophys Mol Biol **2014**;116:101-12
50. Viegas A, Manso J, Nobrega F, Cabrita E. Saturation-Transfer Difference (STD) NMR: A Simple and Fast Method for Ligand Screening and Characterization of Protein Binding. Journal of Chemical Education **2011**;88:990-4
51. Hai T, Wolfgang CD, Marsee DK, Allen AE, Sivaprasad U. ATF3 and stress responses. Gene Expr **1999**;7:321-35
52. De Mol E, Fenwick RB, Phang CT, Buzon V, Szulc E, de la Fuente A, *et al.* EPI-001, A Compound Active against Castration-Resistant Prostate Cancer, Targets Transactivation Unit 5 of the Androgen Receptor. ACS Chem Biol **2016**;11:2499-505
53. Brand LJ, Olson ME, Ravindranathan P, Guo H, Kempema AM, Andrews TE, *et al.* EPI-001 is a selective peroxisome proliferator-activated receptor-gamma modulator with inhibitory effects on androgen receptor expression and activity in prostate cancer. Oncotarget **2015**;6:3811-24
54. Lavery DN, McEwan IJ. Functional characterization of the native NH2-terminal transactivation domain of the human androgen receptor: binding kinetics for interactions with TFIIF and SRC-1a. Biochemistry **2008**;47:3352-9

Figure Legends

Figure 1: UT-155 and UT-69 inhibit AR function and reduce AR expression. A. Structure of UT-155 and UT-69. Ligand binding domain (LBD) binding Ki value is provided below the structure. An AR ligand binding assay was performed with GST-tagged purified human AR-LBD protein and 1 nM ^{3}H mibolerone. **Right table** shows the binding Ki comparison between molecules. **B**. UT-155 and UT-69 inhibit AR transactivation. AR transactivation studies were performed by transfecting human AR cDNA, GRE-LUC, and CMV-renilla LUC into HEK-293 cells. Cells were treated 24 hours after transfection with a dose response of antagonists in combination with 0.1 nM R1881 and a luciferase assay was performed 48 hours after transfection. Values presented are IC_{50}. **C**. UT-155 cross-reacts with progesterone receptor (PR), but minimally with mineralocorticoid receptor (MR) or glucocorticoid receptor (GR). Transactivation was performed by transfecting human AR, PR, GR, or MR cDNA, GRE-LUC, and CMV-renilla LUC into HEK-293 cells. Cells were treated 24 hours after transfection with indicated doses of UT-155 in combination with 0.1 nM R1881 (AR), progesterone (PR), dexamethasone (GR), or aldosterone (MR) and a luciferase assay was performed 48 hours after transfection. **D**. UT-155 and UT-69 potently inhibit the expression of AR-target genes in LNCaP and LNCaP-EnzR cells. LNCaP or LNCaP-EnzR cells were maintained in charcoal stripped serum-containing medium for two days and treated with vehicle or indicated compounds (UT-155, UT-69, or enzalutamide with doses of 1, 10, 100, 1000, and 10,000 nM) in the presence of 0.1 nM R1881 for 24 hours. RNA was isolated and expression of PSA or FKBP5 was quantified and normalized to GAPDH by real time PCR. **E**. UT-155 and UT-69 reduce AR expression. LNCaP cells maintained in charcoal stripped serum-containing medium for 2 days were treated with the indicated doses of UT-155 (left) or 10 μM UT-69 or 10 μM bicalutamide (right) in the presence of 0.1 nM R1881 for ~24 hours. Cells were harvested and a Western blot for the AR was performed with AR-N20 antibody. Actin was used

as a loading control. * significance at p<0.05 from vehicle-treated samples. Enza-enzalutamide; Bical-bicalutamide.

Figure 2. **Distinct requirements for UT-155 and UT-69 to inhibit the AR function. A.** UT-69, but not UT-155, inhibits early induction of NDRG1 and MT2A pre-mRNAs. LNCaP cells maintained in charcoal-stripped serum containing medium for 2 days were treated as indicated in the figures in triplicates. Cells were pre-treated with 10 μM UT-155 or UT-69 for 30 minutes before treatment with 0.1 nM R1881. Cells were harvested, RNA isolated, and the expression of various pre-mRNAs and mRNAs was measured at the indicated time-points. Experiments were repeated three times to confirm the results. * indicates significance at p<0.05 in combination treated samples compared to 0.1 nM R1881-treated samples. **B**. UT-69, but not UT-155, inhibits recruitment of the AR to the androgen response element (ARE). LNCaP cells were serum starved for 2 days and were pre-treated with 10 μM UT-69, UT-155, bicalutamide, or enzalutamide for 30 minutes before treating with 0.1 nM R1881 for 2 hours. DNA-protein complexes were cross-linked and AR was immunoprecipitated and its recruitment to the PSA enhancer ARE was measured by real time PCR. Experiments were performed at n=3 and the results are expressed as mean ± S.E. * indicates significance at p<0.05 in combination-treated samples compared to 0.1 nM R1881-treated samples. Bical – bicalutamide; Enza – enzalutamide.

Figure 3: UT-155 and UT-69 both promote degradation of the AR. **A.** UT-69 and UT-155 do not change AR mRNA levels. LNCaP cells were maintained in charcoal stripped serum-containing medium for two days and treated for 24 hours with vehicle, UT-69, or UT-155 (0.001-10,000 nM) in the presence of 0.1 nM R1881. RNA was isolated and expression of AR or FKBP5 was quantified and normalized to GAPDH by real time PCR. N=3. **B**. UT-155 and UT-69 decrease expression of the AR in LNCaP cells. LNCaP cells maintained in charcoal stripped serum-

containing medium for 2 days were treated with UT-155 (left), UT-69 (middle), and galeterone (right) in the presence or absence of 0.1 nM R1881 for ~24 hours. Cells were harvested and a Western blot for the AR was performed with AR-N20 (left and right) and AR-C-19 (middle) antibodies. Actin was used as a loading control. AR and actin were densitometrically quantified and the level of the AR relative to the level of actin is presented under the blots as fold-change from R1881-treated sample. In the middle panel, 1 nM R1881 and 1 μM UT-69 were used. **C.** UT-155 decreases expression of AR full length in AD1 cells. AD1 cells expressing AR-FL were maintained in charcoal-stripped serum-containing medium for 2 days. Cells were treated for 24 hours, protein extracted, and Western blot for the AR (AR-N20 antibody) and actin was performed. **D**. UT-155 does not reduce PR and ER expression. T47D cells were plated in growth medium and treated with the indicated doses of UT-155. A Western blot for PR, ER, and actin was performed. **E.** UT-155 induces degradation of AR. LNCaP cells were plated in growth medium and treated with 10 μM UT-155, 50 μM cycloheximide, or a combination of UT-155 and cycloheximide for the indicated times. Cells were harvested, protein extracted, and Western blotted for the AR and actin. Results from quantification of the blots (n=3) are provided below. The data were graphed in semi-logarithmic scale and best-fit line was created. **F.** AR degradation by UT-155 could be mediated by proteasome pathway. LNCaP cells maintained in charcoal stripped serum-containing medium for 2 days were treated with vehicle, 10 μM UT-155 alone or in combination with 10 μM MG-132 or 10 μM bortezomib in the presence of 0.1 nM R1881 for 9 hours. Cells were harvested and Western blot for AR and GAPDH was performed. The lanes were densitometrically quantified and the level of the AR relative to the level of GAPDH is presented under the blots as fold-change from R1881-treated sample. Values are expressed as average ± S.E. PR-Progesterone Receptor; csFBS-Charcoal-Stripped FBS; ER-Estrogen Receptor.

Figure 4. UT-155 promotes degradation of AR-SVs. **A.** UT-155 reduces expression of AR and AR-SV in 22RV1 cells. 22RV1 cells maintained in charcoal-stripped serum-containing medium were treated with the indicated doses of UT-155 in the presence of 0.1 nM R1881 for ~24 hours. Cells were harvested and Western blot for AR (AR-N20 antibody) and actin was performed. **Right panels.** UT-155 decreases expression of AR-V567es in D567es cells and AR-SV in LNCaP-95 cells. D567es cells expressing AR-v567es and LNCaP-95 cells expressing AR and AR-SV were maintained in growth medium for 2 days. Cells were treated for 24 hours, protein extracted, and a Western blot for the AR (AR-N20 antibody) and actin was performed. LNCaP-95 experiment was repeated where less protein was loaded on a gel to visualize the degradation of AR full length. **B.** UT-155 induces degradation of AR and AR-SV. 22RV1 cells were plated in growth medium and treated with 10 μM UT-155, 50 μM cycloheximide, or a combination of UT-155 and cycloheximide for the indicated time-points. Cells were harvested, protein extracted, and Western blotted for AR and actin. Results from quantification of the blots are provided as line graphs. The data from three experiments were averaged and plotted on a semi-logarithmic graph and a best fit line was created. **C**. UT-155 inhibits AR-target gene expression in 22RV1 cells. 22RV1 cells were plated in charcoal stripped serum-containing medium, treated with vehicle or the indicated compounds (UT-155 or enzalutamide with 10, 100, 1000, and 10,000 nM) for 48 hours and the expression of FKBP5 was measured by real time PCR. * significance from vehicle-treated samples at $p<0.05$. Enza-enzalutamide SV-splice variant; cyclo/cyclohex-cycloheximide.

Figure 5: UT-155 binds to the AR Activation Function Domain 1 (AF-1) between amino acids 244 and 360. **A.** Steady state fluorescence emission spectra for purified AR-AF1 protein. AR-AF-1 (1 μM) and UT-155 were pre-incubated for at least 30 minutes and steady state fluorescence was measured. The emission spectra were all corrected to buffer alone or buffer with UT-155, as

necessary. **B-E**. Nuclear magnetic resonance (NMR) studies confirm the binding of UT-155 to AR-AF-1. **B.** UT-155 or enzalutamide (500 μM) dissolved in deuterated-d_6DMSO were either added to an NMR tube alone or in combination with 5 μM GST (negative control) or GST-AF-1 purified protein. The intensity of nuclear spin was measured at different magnetic fields (δ ppm). The peaks between 7 and 8 (shown in box) correspond to the aromatic rings of UT-155 and enzalutamide. **C**. WaterLOGSY experiment with UT-155 (200 μM) alone or in combination with 2 μM purified GST-AR-AF-1 was performed as a confirmation for binding. **D**. Map of various N-terminal domain fragments cloned, expressed, and corresponding proteins purified. Purified proteins and molecular weight markers are shown (M.Wt. of fragments=M.Wt.+GST M.Wt. of 26 KDa). **E**. NMR studies were performed with UT-155 (500 μM) and 5 μM of various N-terminal domain fragments as described in panel **B**.

Figure 6. **Characterization of (*R*)-UT-155, which binds only to the AF-1. A.** Amino acids in the AR LBD that interact with UT-155 are important for R1881 transactivation. Molecular modeling shows the critical amino acids in the AR-LBD that interact with UT-155. The amino acids with which UT-155 forms hydrogen bond were mutated and a transactivation assay was performed in HEK-293 cells with R1881 (right). The lower panel shows transactivation assay with wildtype and mutant AR with a dose response of UT-155 in combination with 10 nM R1881. **B.** The *R* isomer of UT-155 inhibits AR transactivation and promotes AR degradation at comparable concentrations, despite lack of binding to the LBD. Structures of S and R isomer of UT-155 are shown. Binding Ki values are provided under the structures. Western blot and transactivation for the AR are shown in the figure. **C.** (*R*)-UT-155 binds to the AR AF-1 domain. (*R*)-UT-155 (500 μM) dissolved in deuterated-d_6DMSO was either added to an NMR tube alone or in combination with 5 μM AF-1 purified protein. The intensity of nuclear spin was measured at different magnetic

fields (δ ppm). The peaks between 6 and 8 (shown by arrows) correspond to the aromatic rings of UT-155. **D**. (*R*)-UT-155 inhibits LNCaP cell growth and R1881-induced FKBP5 gene expression. LNCaP cells plated in RPMI+1%csFBS medium were treated with a dose response of *R*-UT-155 in combination with 0.1 nM R1881. Six days after treatment, with medium changed and re-treated after 3 days, an SRB assay was performed to measure the cell viability. **Bottom**: LNCaP cells were maintained in RPMI+1%csFBS medium for 2 days and treated with a dose response of *R*-UT-155 in the presence of 0.1 nM R1881 for 24 hours. Cells were harvested, RNA isolated, and expression of FKBP5 was measured and normalized to GAPDH. N=3. * indicates significance at $p<0.05$ in combination treated samples compared to 0.1 nM R1881-treated samples.

Figure 7: UT-155 inhibits prostate cancer cell proliferation. **A.** UT-155 is a potent inhibitor of AR-positive prostate cancer cell proliferation. LNCaP, LNCaP-abl, LNCaP-EnzR, or AR-negative Hela cells maintained in charcoal stripped serum containing medium were treated with vehicle or the indicated compounds (1 pM-10 μM for LNCaP and 1-30 μM for other cells) in the presence of 0.1 nM R1881. Cells were re-treated three days later and the cell viability was measured using SRB assay after 6 days of treatment. Values are represented as average ± S.E. with n=3. **B.** UT-155 is a potent inhibitor of AR-SV-expressing prostate cancer cell proliferation. 22RV1 and LNCaP-95 cells were plated in charcoal-stripped serum-containing medium and were treated with the indicated concentrations in the absence of R1881 stimulation. SRB assay was performed 6 days after treatment. **UT-155 inhibits growth of AR- and AR-SV-positive prostate cancer xenografts. C**. UT-155 inhibits growth of LNCaP xenograft. LNCaP cells (5 million/mouse) mixed with matrigel were implanted subcutaneously on the flanks of intact NSG mice (n=6-8 mice/group). Once tumors reached 100-200 mm^3, animals were randomized and treated with vehicle or UT-155 (100 mg/kg/day s.c.). Tumor volume was measured twice weekly. Tumor

weights were recorded at sacrifice. PSA was measured in the protein extracts from the tumors. **D.** UT-155 inhibits growth of 22RV1 xenograft. Xenograft experiment with 22RV1 cells was performed as described in panel A in castrated NSG mice (n=6-8 mice/group). Animals were treated with vehicle, UT-155 (100 mg/kg/day s.c.), or enzalutamide (30 mg/kg/day s.c.). Tumor volume was measured thrice weekly. At sacrifice tumor weights were recorded, protein extracted, and Western blot for AR and actin was performed. PSA was measured in the protein extracts from the tumors. **E.** UT-155 inhibits growth of patient-derived xenograft, Pr-3001. Pr-3001 was implanted as a 1 mm^3 fragment subcutaneously in castrated NSG mice (n=8-10/group) and the study was performed as described above. Tumor volume was measured thrice weekly. * significance at $p<0.05$ from vehicle-treated samples. Enza-enzalutamide. Values are expressed as average ± S.E. of triplicate values. Enza-enzalutamide.

Figure 1

A

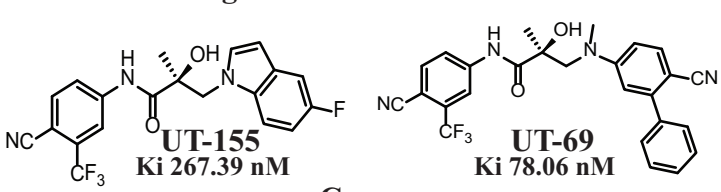

Molecule	Binding Ki (nM)
Enzalutamide	3641.29
Galeterone	2648.56
Apalutamide	1452.29
UT-155	267.39
UT-69	78.06

B

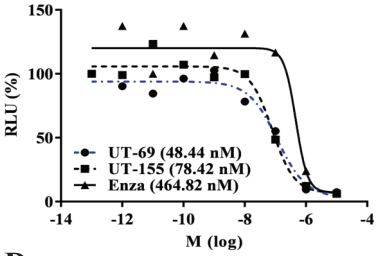

C

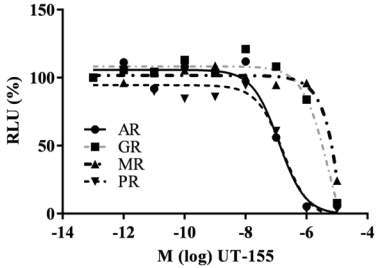

D

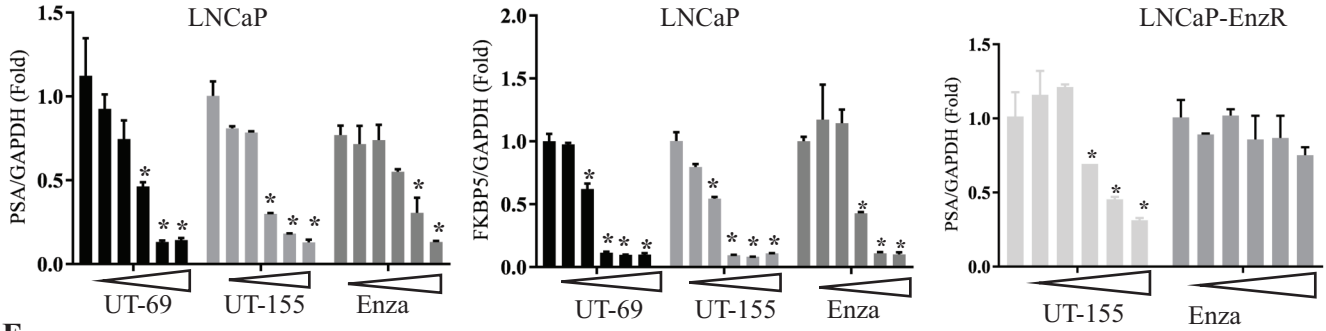

E

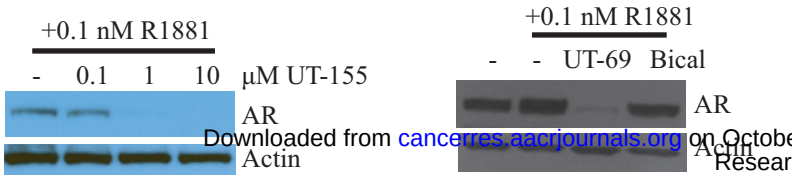

Figure 2

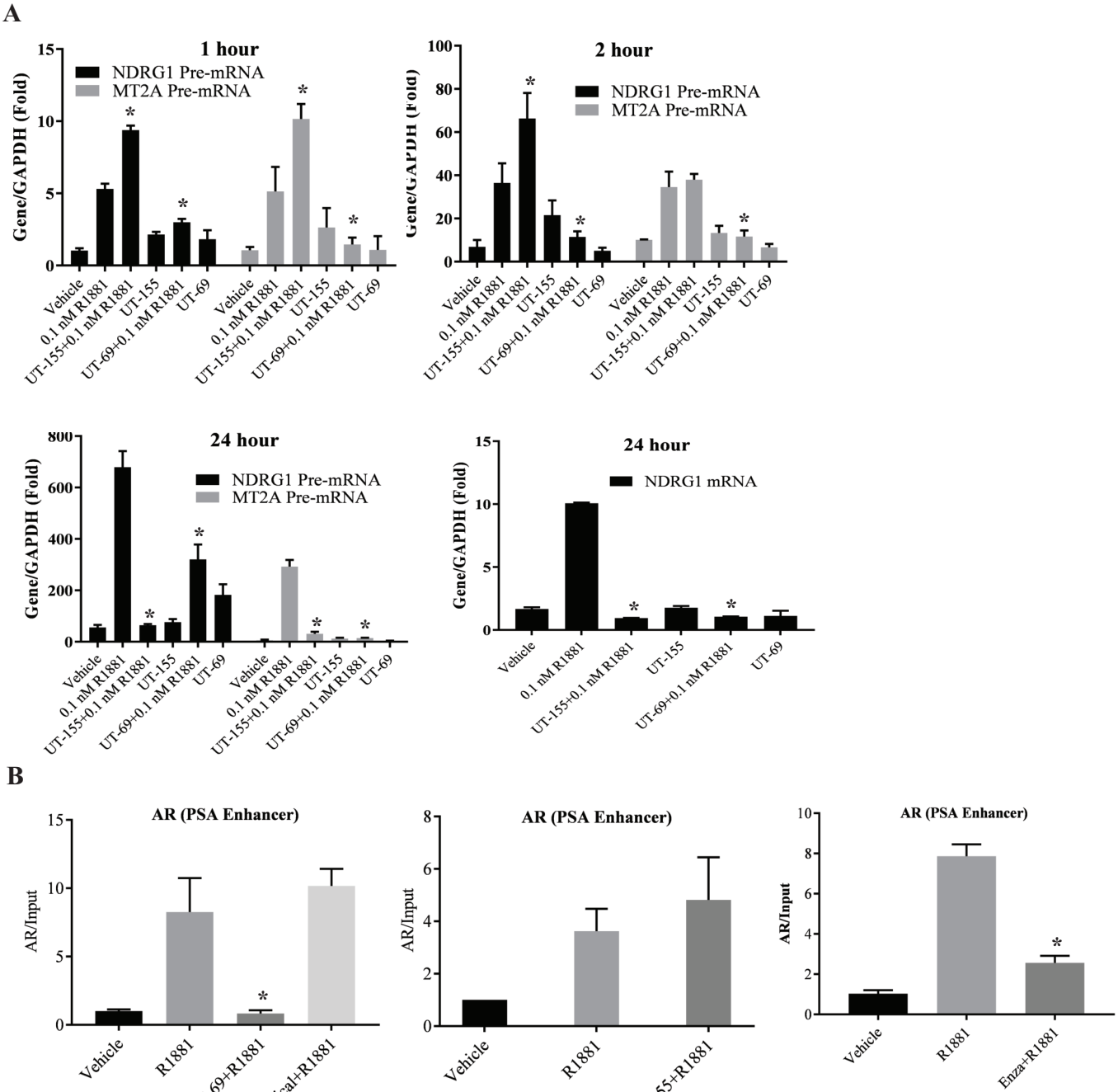

Figure 3

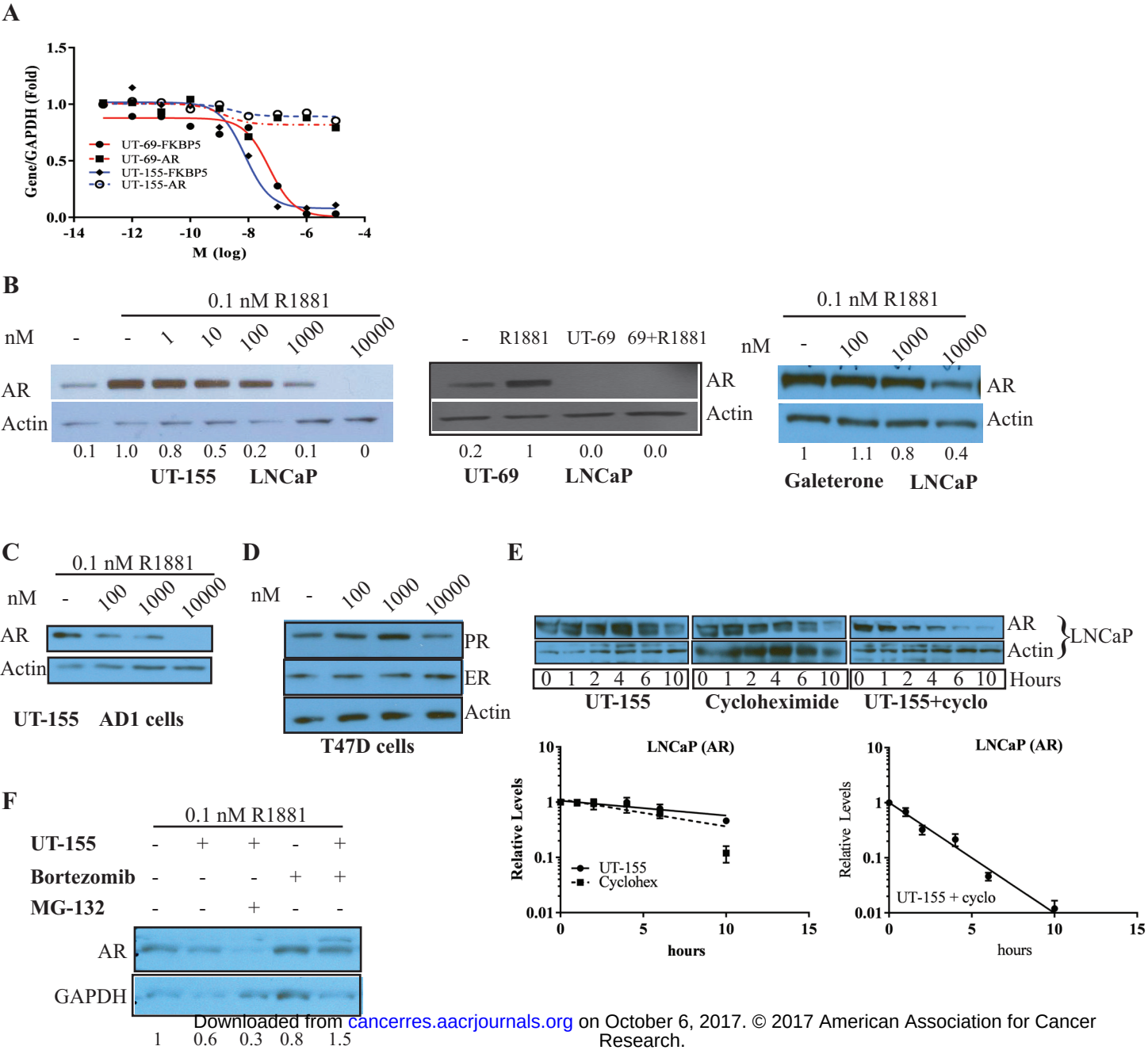

Figure 4

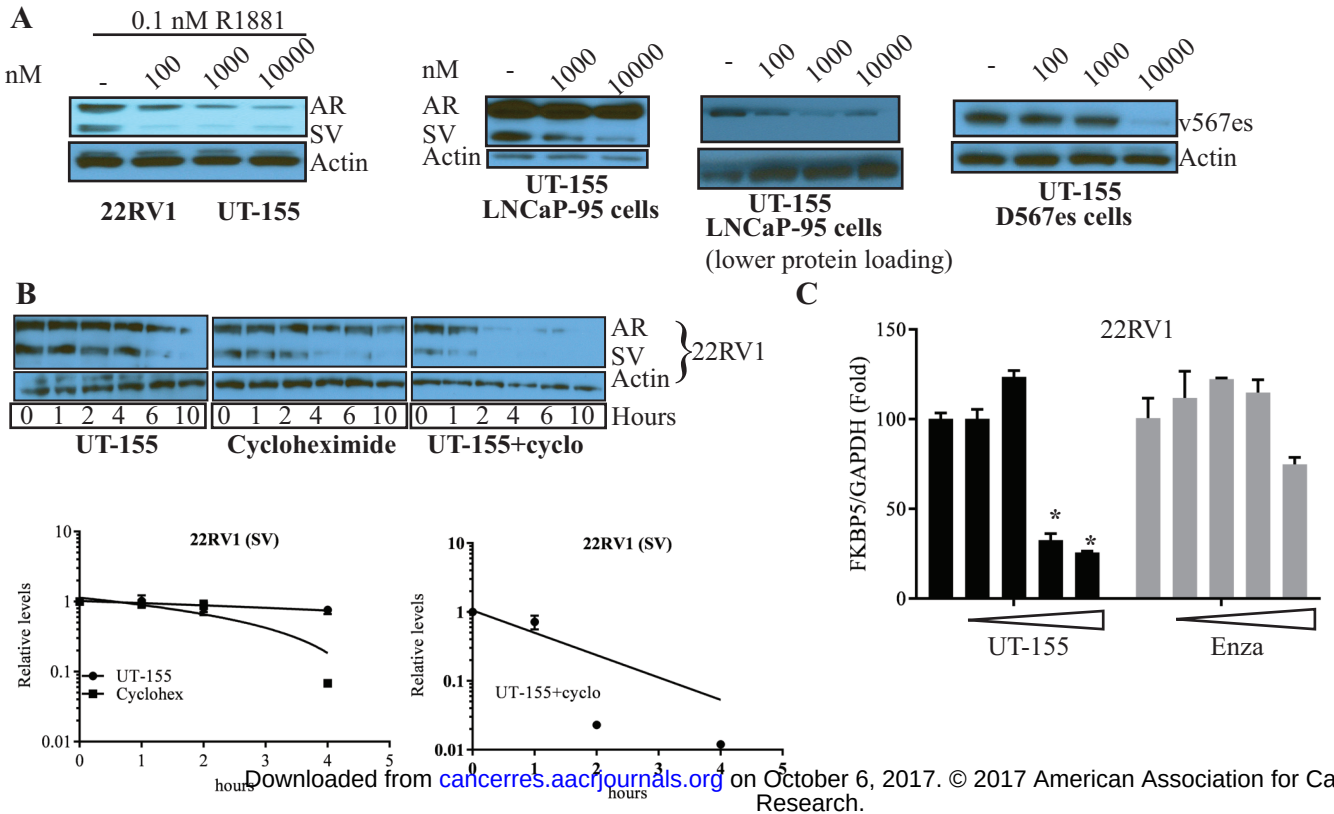

Author Manuscript Published OnlineFirst on October 4, 2017; DOI: 10.1158/0008-5472.CAN-17-0976
Author manuscripts have been peer reviewed and accepted for publication but have not yet been edited.

Figure 5

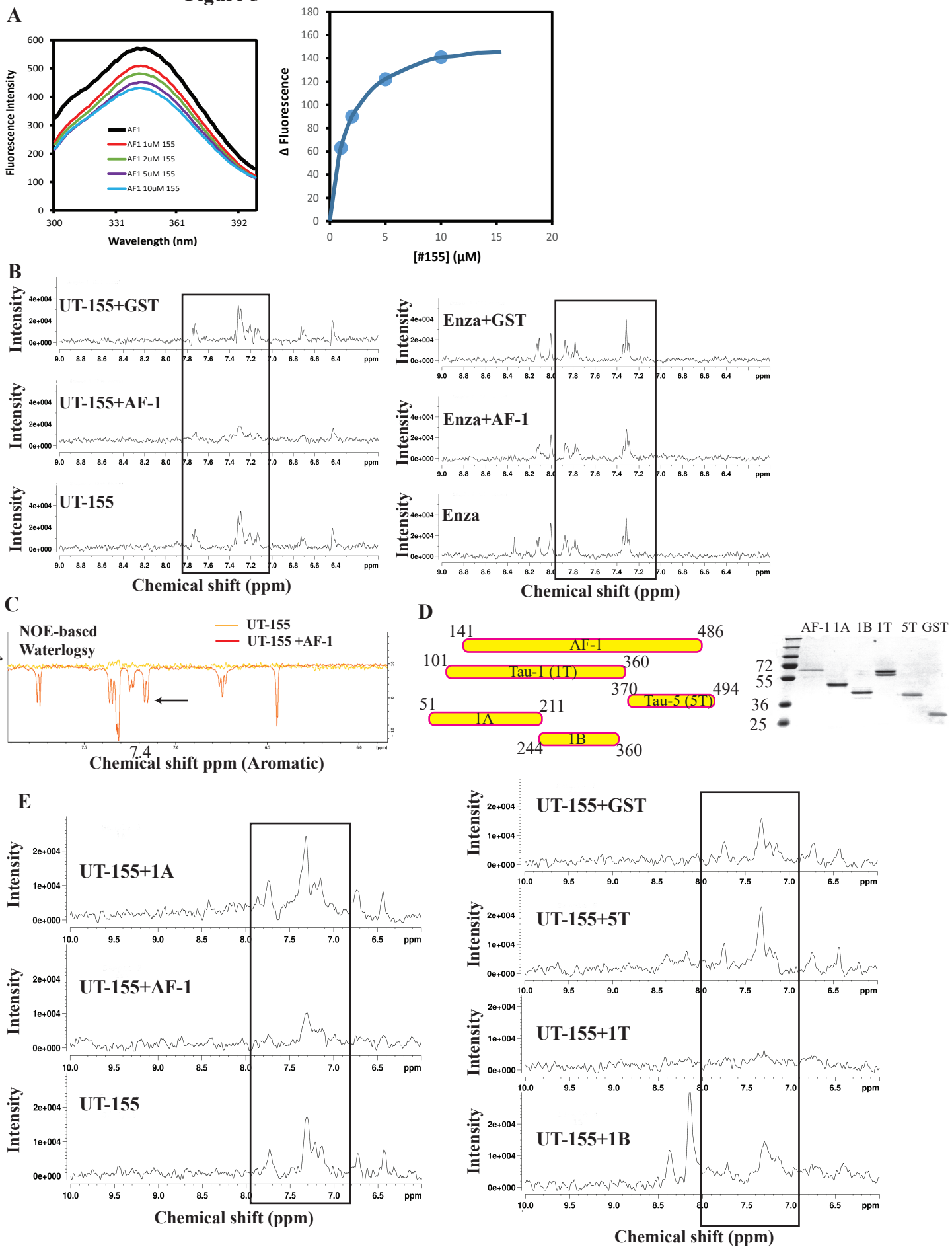

Figure 6

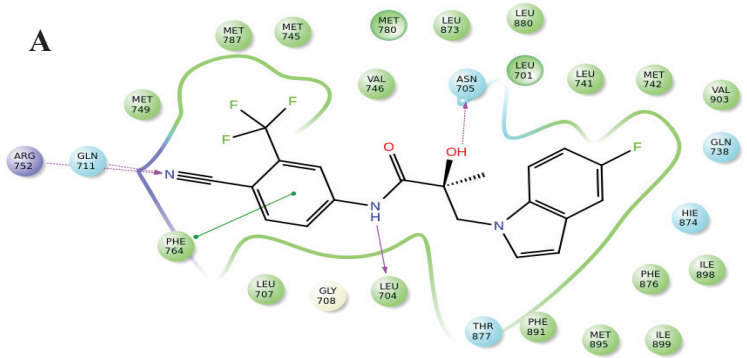

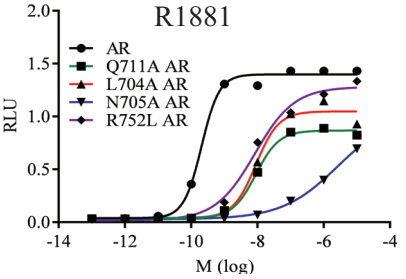

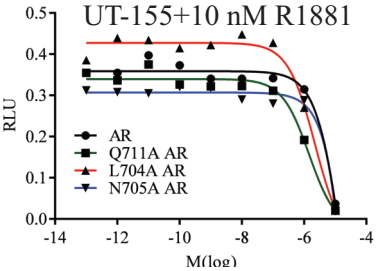

B

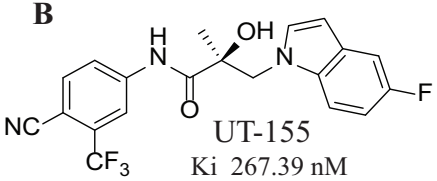

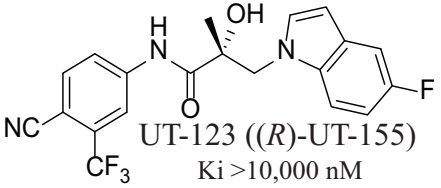

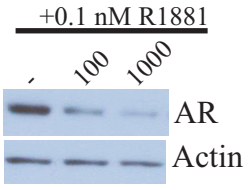

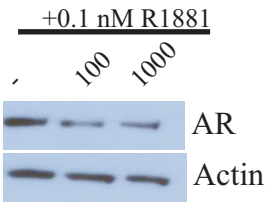

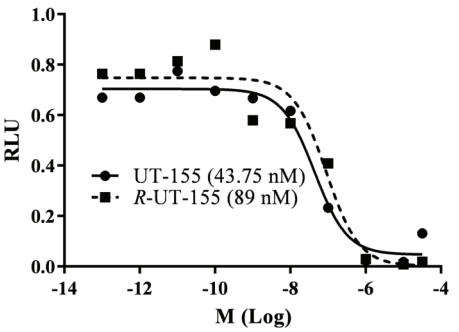

C

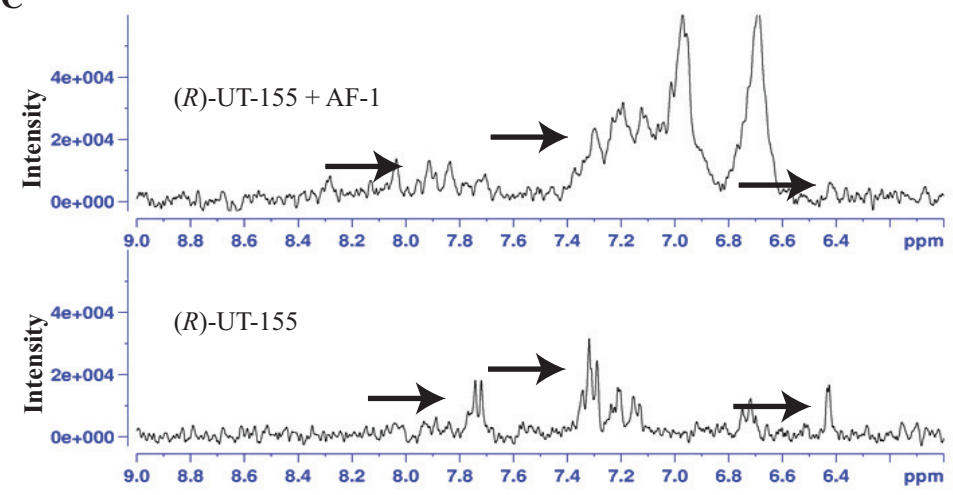

D

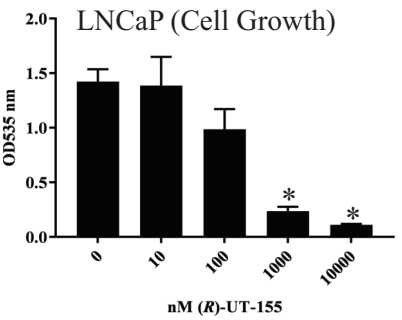

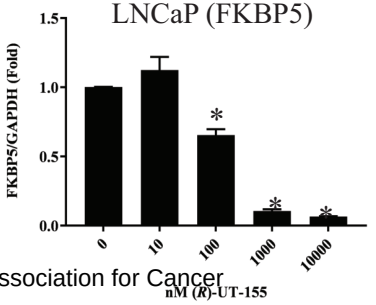

Figure 7

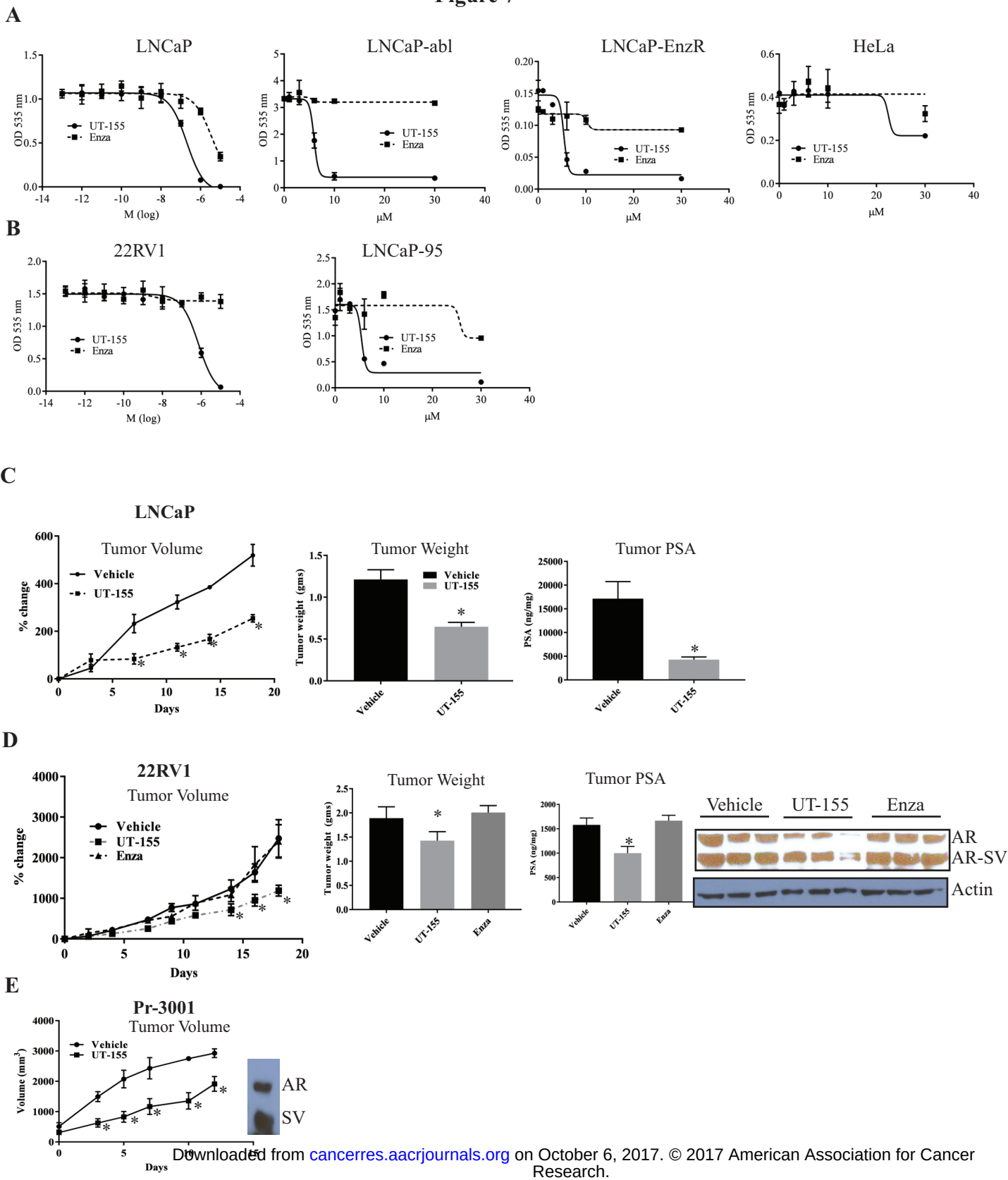

AACR American Association for Cancer Research

Cancer Research

The Journal of Cancer Research (1916–1930) | The American Journal of Cancer (1931–1940)

Novel selective agents for the degradation of androgen receptor variants to treat castration-resistant prostate cancer

Suriyan Ponnusamy, Christopher C Coss, Thirumagal Thiyagarajan, et al.

Cancer Res Published OnlineFirst October 4, 2017.